

Unveiling the Nature of Giant Ellipticals and their Stellar Halos with the VST

Marilena Spavone¹
 Massimo Capaccioli^{1,2}
 Nicola R. Napolitano¹
 Enrichetta Iodice¹
 Aniello Grado¹
 Luca Limatola¹
 Andrew P. Cooper³
 Michele Cantiello⁴
 Duncan A. Forbes⁵
 Maurizio Paolillo²
 Pietro Schipani¹

¹ INAF–Astronomical Observatory of Capodimonte, Italy

² University of Naples Federico II, Italy

³ Institute for Computational Cosmology, Durham, United Kingdom

⁴ INAF–Astronomical Observatory of Teramo, Italy

⁵ Centre for Astrophysics & Supercomputing, Swinburne University, Australia

Observations of diffuse starlight in the outskirts of galaxies provide fundamental constraints on the cosmological context of galaxy assembly in the Lambda Cold Dark Matter model, which predicts that galaxies grow through a combination of *in-situ* star formation and accretion of stars from other galaxies. Accreted stars are expected to dominate in the outer parts of galaxies. Since dynamical timescales are longer in these regions, substructures related to accretion, such as streams and shells, can persist over many Gyr. In this work we use extremely deep *g*- and *i*-band images of six massive early-type galaxies (ETGs) from the VEGAS survey to constrain the properties of their accreted stellar components. The wide field of view of OmegaCAM on the VLT Survey Telescope (VST) also allows us to investigate the properties of small stellar systems (such as globular clusters, ultra-compact dwarfs and satellite galaxies) in the halos of our galaxies. By fitting light profiles, and comparing the results to simulations of elliptical galaxy assembly, we have identified signatures of a transition between relaxed and unrelaxed accreted components and can constrain the balance between *in-situ* and accreted stars.

Early-type galaxy stellar halos

The Lambda Cold Dark Matter (Λ CDM) galaxy formation theories predict that galaxies grow through a combination of *in-situ* star formation and accretion of stars from other galaxies. Accreted stars are expected to dominate in the outer parts of galaxies because they have much lower binding energies in the remnant system than stars formed by dissipative collapse. The structural properties of the outer parts of galaxies and their correlations with stellar mass and other observables might therefore provide ways of testing theoretical predictions of growth by accretion.

Cosmological simulations of galaxy formation predict trends in these quantities with mass that lead to systematic variations in the average shape, amplitude, and extent of azimuthally averaged surface brightness profiles (Cooper et al., 2013). Unfortunately, the accreted debris is also expected to have extremely low surface brightness ($\mu_v \sim 29$ mag arcseconds⁻²) on average and therefore to be very hard to separate from the background sky in conventional photometric observations. In theoretical models massive ETGs accumulate the bulk of their stellar mass by accretion, predominantly through about ten mergers of low stellar mass ratio (Cooper et al., 2015).

From an observational perspective, the connections between different mechanisms of mass growth and the “structural components” inferred from images of ETGs are not straightforward. If the bulk of the stars really are accreted, then the “stellar halo” should be identified with at least the structural component that dominates the observed stellar mass. However, other empirical components might also be accreted. *In-situ* stars in ETGs are extremely difficult to distinguish if they are also spheroidal and dispersion-supported and have old, metal-rich stellar populations resembling those of the dominant accreted component(s) with which they have been thoroughly mixed by violent relaxation.

Cosmological dynamical simulations can help by suggesting plausible interpretations for features in the surface brightness profiles of ETGs in the context of

specific galaxy formation theories. In particular, simulated galaxies show evidence of substructure in the form of inflections or breaks, at which the surface brightness profile becomes either steeper or shallower (for example, Cooper et al., 2013; Rodriguez-Gomez et al., 2016). These inflections also correspond to variations in the ratio between individual accreted components as a function of radius. Most simulations predict that the transition between *in-situ* and accretion-dominated regions should be almost imperceptible in the azimuthally averaged profiles of typical ETGs.

Observational work has clearly identified features in ETG surface brightness profiles and kinematic distributions that are indicative of substructure in the accreted component (Bender et al., 2015). Some of these features occur at distances of many effective radii and hence at very low surface brightness, which could be interpreted as evidence for multiple accreted components in the context of the models mentioned above. Using different techniques with observations of different depths, several authors have concluded that the profiles of massive ETGs are not well described by a single Sérsic law component, once thought to be near universal for spheroidal galaxies, suggesting that three or more Sérsic components may be required for an accurate description of typical ETGs.

The VEGAS survey

The study of galaxy stellar halos, historically hampered by their faintness, has recently benefited from the new generation of very-wide-field imaging instruments. We are taking advantage of the wide field of view and high spatial resolution of the VLT Survey Telescope (VST) at ESO’s Paranal Observatory to carry out a multi-band imaging survey of nearby ETGs, named VEGAS (VST Early-type GALaxies Survey; Capaccioli et al., 2015). The large field of view of the OmegaCAM mounted on the VST (one square degree matched by pixels 0.21 arcseconds wide), together with its high efficiency and spatial resolution, allows us to map the surface brightness of a galaxy out to isophotes encircling about 95% of the total light using a reasonable integration.

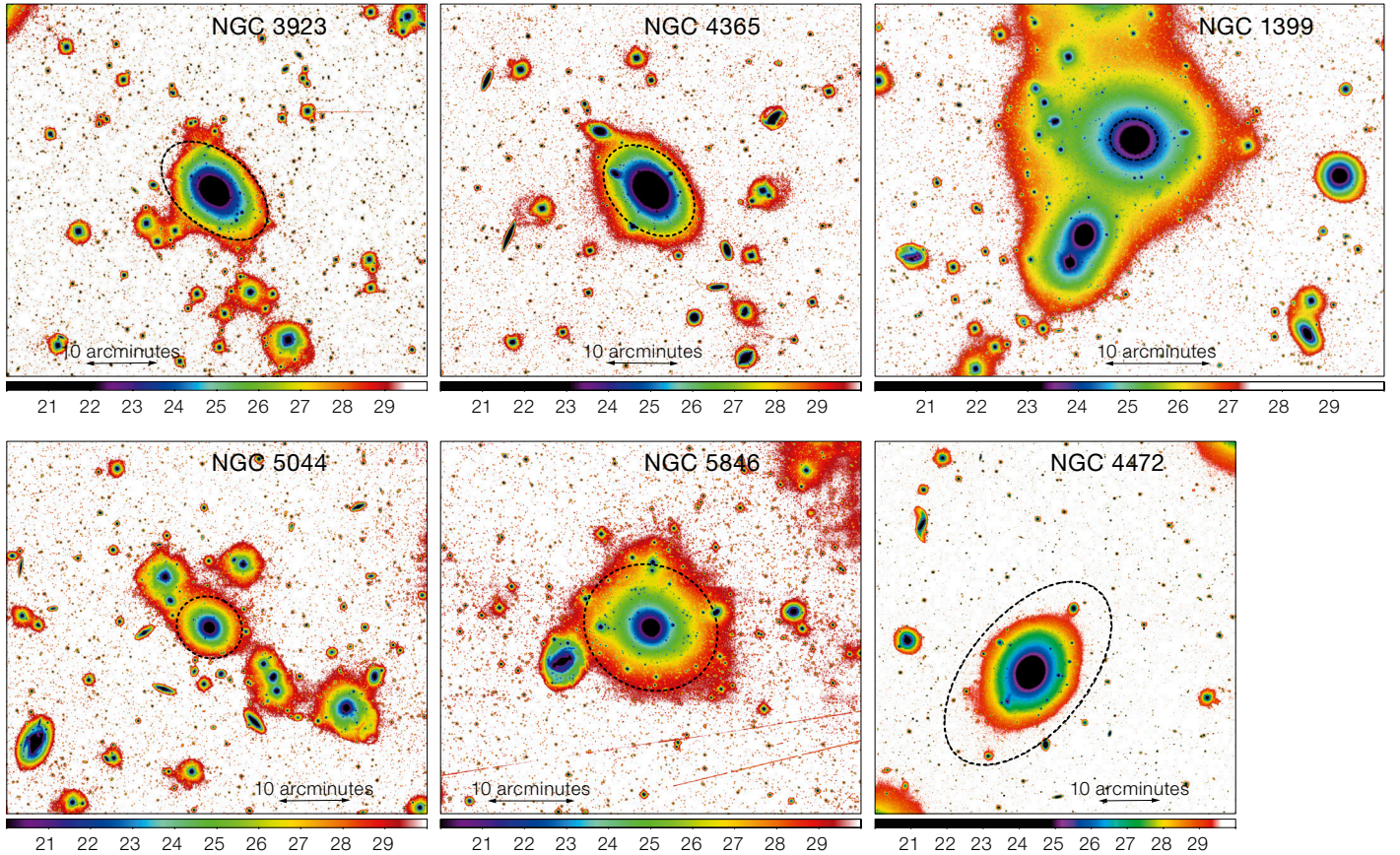


Figure 1. VST g -band sky-subtracted images of the galaxies analysed in this work. The colour scale represents surface brightness in $\text{mag arcseconds}^{-2}$. North is up, east is to the left. We point out that the stellar halos often extend even further than it is possible to visualise in these images, as shown by the profiles in Figure 3.

The main products of the VEGAS survey are: 1) a two-dimensional light distribution out to 8–10 effective radii (R_e), galaxy structural parameters and diffuse light component, inner substructures as a signature of recent cannibalism events; 2) radially-averaged surface brightness profiles and isophote shapes out to $10 R_e$; 3) colour gradients and the connection with galaxy formation theories; 4) detection of external low-surface-brightness structures of the galaxies and the connection with the environment; and 5) a census of small stellar systems (globular clusters, ultra-compact dwarfs and galaxy satellites) out to $\sim 20 R_e$ from the main galaxy centre and their photometric properties.

The data used in this work consist of exposures in g and i Sloan Digital Sky

Survey bands obtained with VST and OmegaCAM, in both service and visitor mode, for the giant ETGs (Figure 1) NGC 3923, NGC 4365, NGC 5044 and NGC 5846, along with similar data on NGC 4472 and NGC 1399 (Capaccioli et al., 2015 and Iodice et al., 2016).

The data reduction procedure followed is described by Capaccioli et al. (2015) and Spavone et al. (2017). We adopted a “step-dither” observing strategy for galaxies with large angular extents, consisting of a cycle of short exposures centred on the target and on offset fields ($\Delta = \pm 1$ degree). With such a technique the background can be estimated from exposures taken as close as possible, in space and time, to the scientific images. This ensures better accuracy, reducing the uncertainties at very faint surface brightness levels.

Results

The isophotal analysis of the VEGAS galaxies is performed on the final mosaic in

each band with the IRAF task ELLIPSE, which computes the intensity, $I(a, \theta)$, azimuthally sampled along an elliptical path described by an initial guess for the isophote centre (X, Y) , ellipticity ϵ , and semi-major axis position angle θ at different semi-major axis lengths.

We find an increase in ellipticity in the outer regions of all the galaxies, indicating the presence of a more flattened outer component with a significant gradient in position angle. From the isophotal analysis we also extract very deep surface brightness profiles ($\mu_g \sim 30 \text{ mag arcseconds}^{-2}$). In the left panel of Figure 2 we plot these profiles as a function of galactocentric radius normalised to the effective radius R/R_e . This comparison shows that we have two kinds of profiles in our sample: those with “excess” light in the outer regions, which tend to flatten in these regions; and those for which the surface brightness falls off more rapidly. The differences in the shape of the light profiles may be signatures of different dynamical states for the stellar halos surrounding

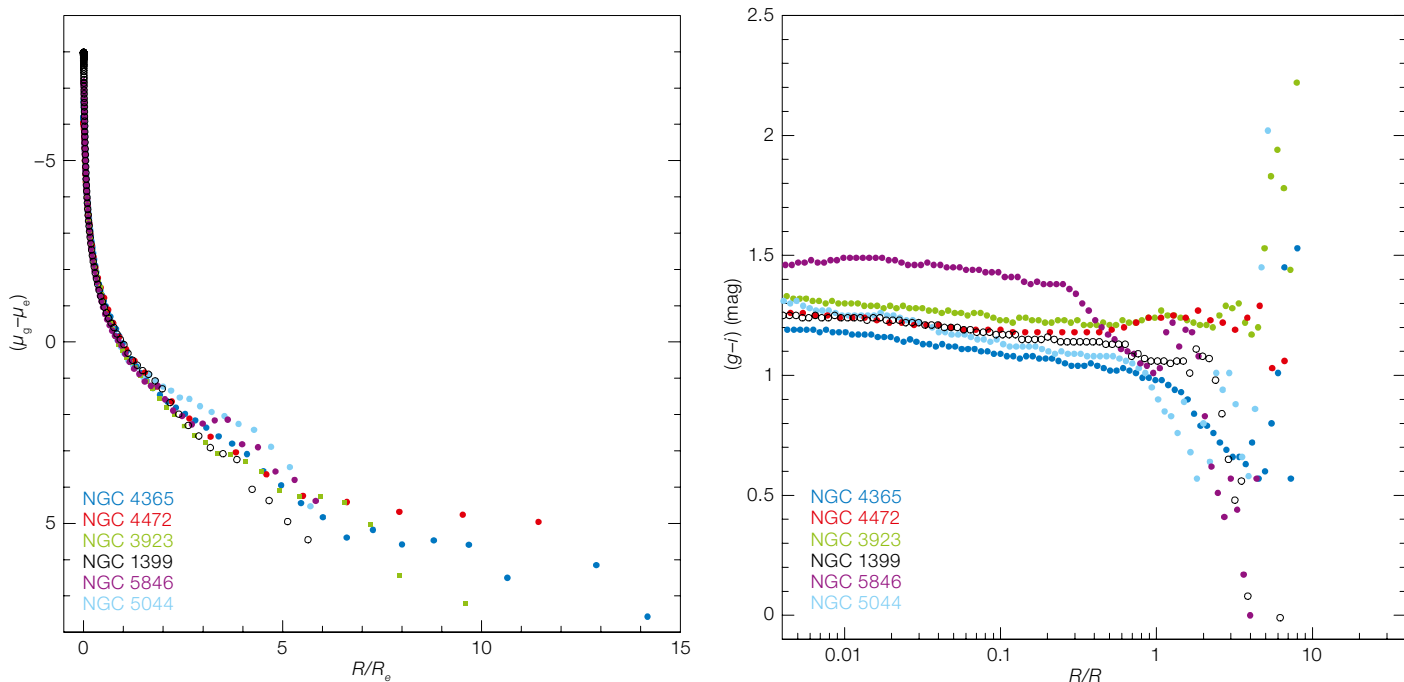


Figure 2. Left: Azimuthally-averaged surface brightness profiles in the g -band scaled to their effective magnitude, as a function of galactocentric radius normalised to the effective radius, R/R_e . Right: The $(g-i)$ colour profiles of the galaxies in our study.

these galaxies. The mean $(g-i)$ colour profiles for galaxies in our sample are shown in the right panel of Figure 2. The colours of all our galaxies are redder than those typically found for ETGs, since they all show the presence of dust lanes, shells, and other signs of ongoing interactions. The colours develop a steeper gradient at a different radius for each galaxy, becoming bluer (for NGC 1399, NGC 4365, NGC 5044 and NGC 5846) or redder (for NGC 3923 and NGC 4472). We will show later that the discontinuities observed in the colour profiles, ellipticities and position angles correspond to the transition radii observed in each surface brightness profile, which are defined as the locations of the transition between two different fit components.

Since there is considerable evidence in the literature that the light profiles of many of the most massive ETGs are not fitted well by a single Sérsic law and at least one additional component is needed (Seigar et al., 2007; Donzelli et al., 2011), our analysis focuses on the fit of projected one-dimensional (ellipsoidally averaged)

surface brightness profiles of our sample galaxies. This second component is sometimes interpreted as evidence for a stellar halo. The overall profile is composed of different contributions and therefore theory suggests that the surface brightness profiles of ETGs should be described by the superposition of different components. For this reason, we first present models of the surface brightness profiles of galaxies in our sample with a double Sérsic law (r^{-n}), or with an exponential profile ($n = 1$) on the outer component. The result of these fits and their residuals are shown in Figure 3.

From this analysis we have identified a radius for each galaxy in our sample that marks the transition between the inner and outer components of our two-component fit. We label this empirically defined “transition radius” R_{tr} . This transition occurs at very faint levels of surface brightness (μ_{tr}) for all our galaxies. Moreover, a discontinuity in the ellipticity, position angle, and $(g-i)$ colour profile of each of the six galaxies occurs around R_{tr} (see Spavone et al., 2017).

The relative contribution of the outer halo with respect to the total galaxy light (f_{h1}) estimated from these fits ranges from 27% to 64%. Since there is no clear reason to believe that the outer component

in a fit such as this accounts for most of the accreted mass in massive elliptical galaxies, these halo mass fractions should be considered a lower limit for the total accreted mass.

Numerical simulations predict that stars accreted by brightest cluster galaxies (BCGs) account for most of the total galaxy stellar mass ($\sim 90\%$ on average), while *in-situ* stars only contribute significantly to the surface brightness profiles out to $R \sim 10$ kpc (Cooper et al., 2013, 2015; Rodriguez-Gomez et al., 2016). The overall accreted profile is built up of contributions from several significant progenitors. For this reason, theory suggests that the surface brightness profile of an ETG should be well described by the superposition of an inner Sérsic profile, representing the sub-dominant *in-situ* component in the central regions, with another Sérsic profile representing the dominant superposition of the relaxed phase-mixed accreted components, and an outer diffuse component representing unrelaxed accreted material (streams and other coherent concentrations of debris), which does not contribute significant surface density to the brighter regions of the galaxy.

Following these theoretical predictions, we described the surface brightness

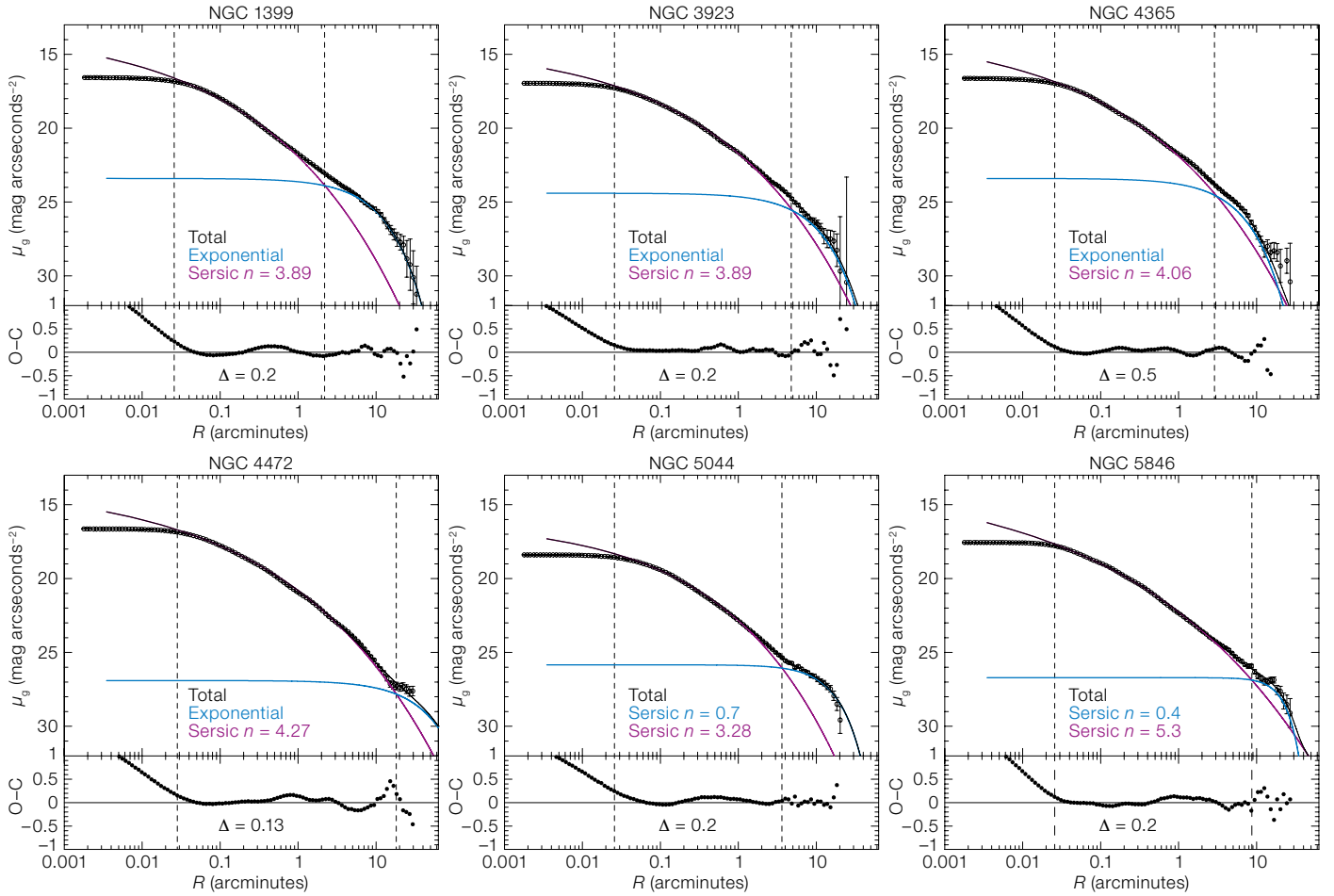


Figure 3. VST g -band profiles of NGC 1399, NGC 3923, NGC 4365, NGC 4472, NGC 5044, and NGC 5846 plotted on a logarithmic scale. The blue line is a fit to the outer regions, while the magenta line is a fit to the inner regions with a Sérsic profile, and the black line is the sum of the components in each fit. The dashed lines indicate the core of the galaxy, which was excluded from the fit, and the transition point between the two components, respectively.

profiles of our six galaxies with a three-component model: a Sérsic profile for the centrally concentrated *in-situ* stars, a second Sérsic for the relaxed accreted component, and an exponential component for the diffuse and unrelaxed outer envelope. To mitigate the degeneracy in parameters and provide estimates of accreted components that are closely comparable to the results of numerical simulations, we fixed $n \sim 2$ (allowing small variations of ± 0.5) for the *in-situ* component of our three-component fits (Cooper et al., 2013). The results of these fits are shown in Figure 4. From this plot it

appears that, as argued by Cooper et al. (2015), the radius R_{tr} identified in Figure 2 marks the transition between different accreted components in different states of dynamical relaxation, rather than between *in-situ* and accreted stars. From the fitting procedure we estimated the contributions of the outer exponential “envelopes” to the total galaxy mass; these range from 28% to 60% for the galaxies in our sample. We also estimate the fractions of total accreted mass, which range from 83% to 95%.

Comparison with theoretical predictions

In the previous section, we identified inflections in the surface brightness profiles of galaxies in our sample that may correspond to transitions between different accreted progenitors in different dynamical states. In Figure 5 we compare the accreted mass ratios inferred from

our observations (filled red triangles) with other observational estimates for BCGs (Bender et al., 2015; Seigar et al., 2007; Iodice et al., 2016), with theoretical predictions from semi-analytic particle-tagging simulations by Cooper et al. (2013, 2015), and with the Illustris cosmological hydrodynamical simulations (Rodríguez-Gomez et al., 2016).

We find that the stellar mass fraction of the accreted component derived for galaxies in our sample is fully consistent with both published data for other BCGs (despite considerable differences in the techniques and assumptions involved) and the theoretical models of Cooper et al. (2013, 2015). In Figure 5 we also compare the stellar mass fractions obtained for the outermost exponential component of our multi-component fit (open red triangles) with the mass fraction associated with unbound debris streams from surviving cluster galaxies in the simulations of Cooper et al. (2015). We found that the

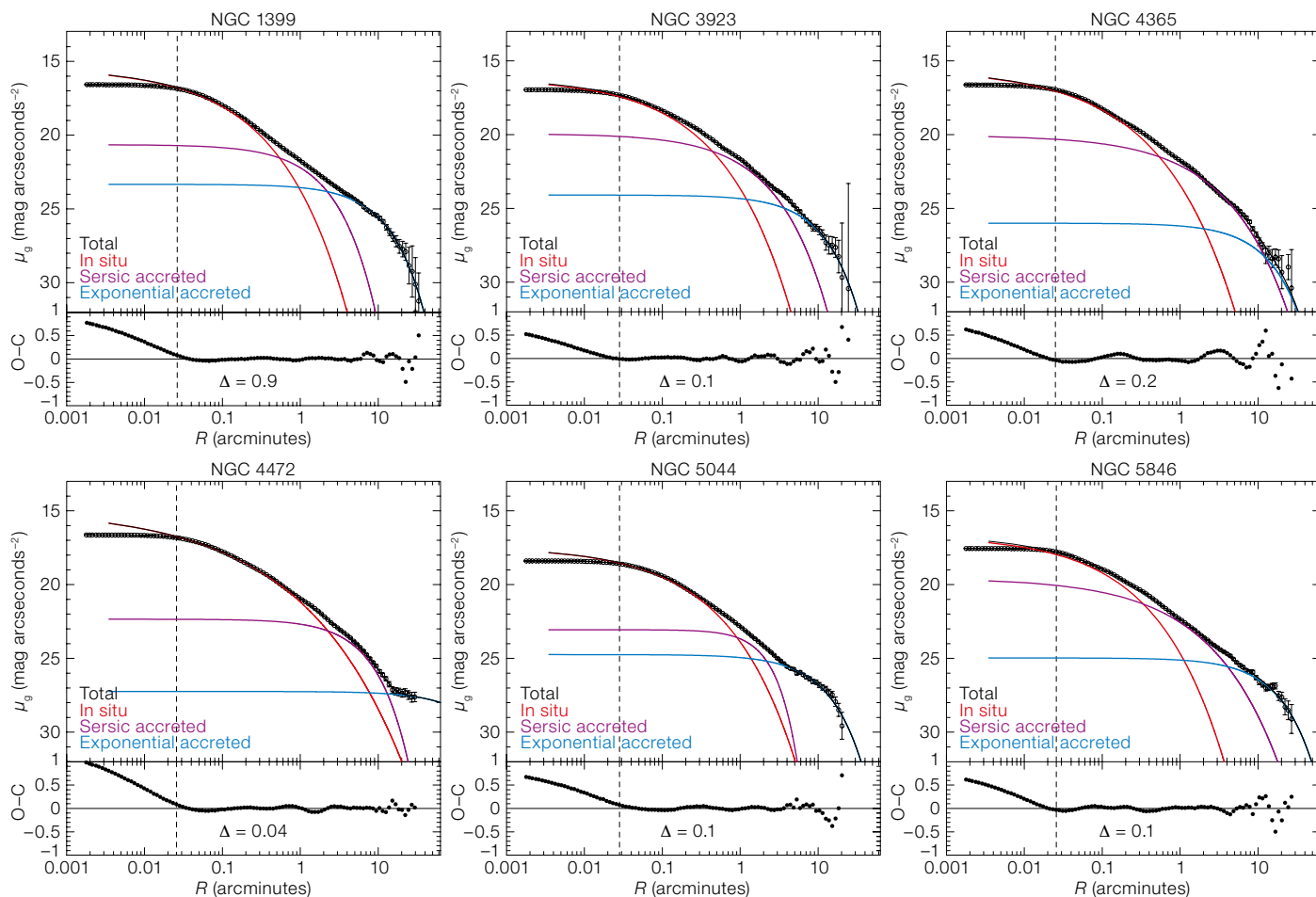


Figure 4. VST g -band profiles of NGC 1399, NGC 3923, NGC 4365, NGC 4472, NGC 5044, and NGC 5846, fitted with a three-component model motivated by the predictions of theoretical simulations.

mass fraction in this component of our fits is consistent with these values from the simulations, suggesting that such components may give a crude estimate of the mass distribution associated with dynamically unrelaxed components originating from disrupting or recently disrupted galaxies, as argued by Cooper et al. (2015).

Clues to the origin of stellar halos

Our analysis suggests that the surface brightness profiles of the galaxies in our study are best reproduced by multi-component models. For each of the galaxies in our study we can identify at least one inflection in the surface brightness profile. These inflections occur at very faint surface brightness levels

($24.0 \leq \mu_g \leq 27.8 \text{ mag arcseconds}^{-2}$).

They appear to correlate with changes in the trend of ellipticity, position angle, and colour with radius, where the isophotes become flatter and misaligned and the colours become bluer beyond the inflections. This suggests that these inflections mark transitions between physically distinct components in different states of dynamical relaxation.

A variety of possible interpretations for such features have been suggested, based on theoretical models. Upward inflections (shallower outer slopes) might reflect transitions between either an inner *in-situ*-dominated region and an outer accretion-dominated region, or else between two accreted components (Font et al., 2011). Downward inflections can occur within the profiles of debris from single progenitors alone, corresponding to the characteristic apocentric radius of its stars (Cooper et al., 2010; Deason et al., 2013) and therefore need not represent

a transition between two separate components. We do not observe significant changes in surface brightness or other properties at the transition point between the inner two components of our theoretically motivated three-component fits. This is perhaps not surprising because simulations predict that the *in-situ* accreted transition is hardly noticeable in very massive galaxies, for the most part because the *in-situ* stars account for a relatively small fraction of the total mass even in the bright body of the galaxy. It is encouraging that we see a variety of profile inflections in our photometric investigation of this small subset of the VEGAS sample and that these are broadly consistent with expectations based on state-of-the-art theoretical models.

Our results suggest that, with the complete sample of extremely deep surface brightness profiles from the full survey, we will be able to investigate the late stages of massive galaxy assembly statistically,

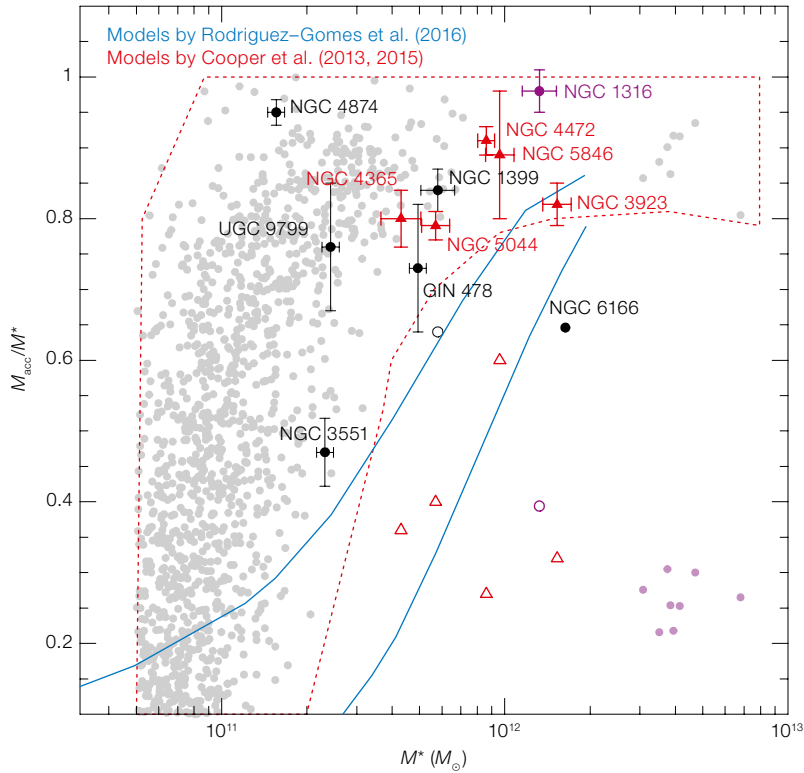


Figure 5. Accreted mass fraction versus total stellar mass for ETGs. Our VEGAS measurements are given as red filled and open triangles (see text for details). Black circles correspond to other BCGs from the literature. Red and blue regions indicate the predictions of cosmological galaxy formation simulations

by Cooper et al. (2013, 2015) and Rodriguez-Gomez et al. (2016), respectively. Purple-grey points show the mass fraction associated with the streams from Table 1 in Cooper et al. (2015) for comparison to the observations shown by open symbols.

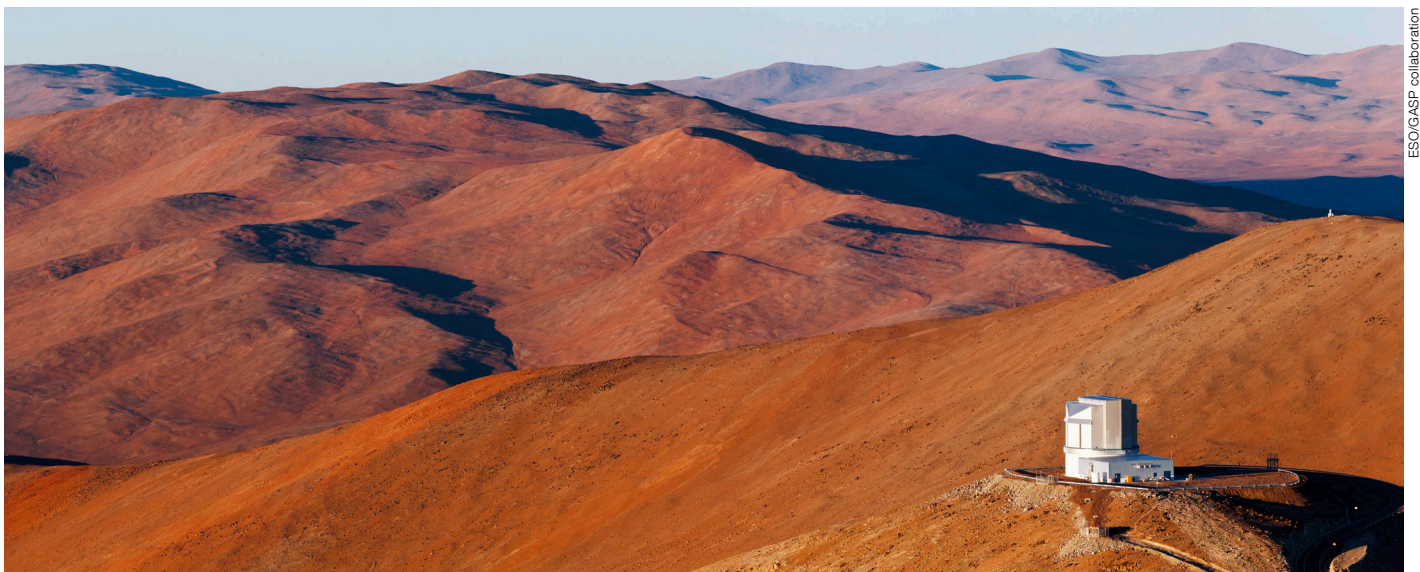
thereby distinguishing dynamically evolved systems from those that are still reaching dynamical equilibrium, and probing the balance between *in-situ* star formation and accretion across a wide range of stellar mass. This is a promising route to constraining cosmological models of galaxy formation such as those we have compared with here, which predict fundamental, relatively tight correlations between the present-day structure of massive galaxies and the growth histories of their host dark matter halos.

Acknowledgements

M. Spavone wishes to thank the ESO staff for their support during the observations at the VST. The data reduction for this work was carried out with the computational infrastructure of the INAF-VST Center at Naples (VSTceN). M. Spavone acknowledges financial support from the VST project (PI M. Capaccioli).

References

- Bender, R. et al. 2015, ApJ, 807, 56
- Capaccioli, M. et al. 2015, A&A, 581, A10
- Cooper, A. P. et al. 2013, MNRAS, 434, 3348
- Cooper, A. P. et al. 2015, MNRAS, 451, 2703
- Deason, A. J. et al. 2013, ApJ, 763, 113
- Donzelli, C. J. et al. 2011, ApJ, 195, 15
- Font, A. S. et al. 2011, MNRAS, 416, 2802
- Iodice, E. et al. 2016, ApJ, 820, 42
- Rodriguez-Gomez, V. et al. 2016, MNRAS, 458, 2371
- Seigar, M. S. et al. 2007, MNRAS, 378, 1575
- Spavone, M. et al. 2017, A&A, 603A, 38S



ESO/GASP collaboration

The Visible and Infrared Survey Telescope for Astronomy (VISTA).